

# Clouds and Hazes in the Atmospheres of Triton and Pluto

Peter Gao<sup>1</sup> and Kazumasa Ohno<sup>2</sup>

<sup>1</sup>Earth & Planets Laboratory, Carnegie Institution for Science, Washington, DC, USA

<sup>2</sup>Division of Science, National Astronomical Observatory of Japan, Tokyo, Japan  
pgao@carnegiescience.edu

## 1 Introduction

Clouds and hazes are abundant in the thin ( $\sim 10 \mu\text{bar}$ ) and cold ( $\leq 40 \text{ K}$ ) atmospheres of Triton and Pluto, where they are thought to be produced by interactions between atmospheric gases and ultraviolet (UV) photons from the Sun and those scattered by the local interstellar medium. These interactions lead to a rich network of chemical reactions that produces higher order hydrocarbons and nitriles that condense out to form ice clouds, and ultimately complex haze particles that rain down onto the surface that impact the atmospheric thermal structure, gas chemistry, and surface evolution. In this chapter, we will review the observational evidence for clouds and hazes in the atmospheres of Triton and Pluto and theoretical interpretations thereof, and the emerging set of experiments aiming to produce Triton and Pluto clouds and hazes in the lab to learn about them in detail.

### 1.1 A Note on Nomenclature

It is important to give formal definitions to “clouds” and “hazes”, as their definitions vary between Earth and planetary science literature. Here we will follow the latter and use definitions related to provenance: *Cloud* particles form through equilibrium condensation reactions, where the local temperature and condensate vapor abundance are such that condensation is energetically favorable and occurs spontaneously. In contrast, *haze* particles form through disequilibrium processes, typically photochemical reactions, where injection of energy (e.g. UV photons) breaks apart atmospheric gas molecules and leads to reactions that gradually build the haze particles. As a result, cloud particles are typically volatile while haze particles are typically not. A complication of these definitions involves particles that form from condensation of gases that were themselves produced photochemically; while we will refer to these structures as clouds here, they have also been referred to as hazes in the literature. Finally, we will use “aerosols” as a catch-all term for any particulates suspended in an atmosphere, i.e. both clouds and hazes<sup>1</sup>, in cases where the provenance is uncertain.

## 2 Observations of Triton and Pluto Aerosols

### 2.1 Voyager 2 Observations of Triton Aerosols

Voyager 2’s historic flyby of the Neptune system on 25 August 1989 revealed the existence of a  $\text{N}_2$ -dominated atmosphere on Triton with surface pressure and temperature of  $16 \pm 3 \mu\text{bar}$  and  $38_{-4}^{+3} \text{ K}$ , respectively, consistent with conditions of vapor equilibrium with surface  $\text{N}_2$  ice [3,79,8]. The observed near-surface mixing ratio of  $\text{CH}_4$  (few to a few hundred ppm) was subsaturated by a factor of 30 and spatially variable with a scale height of 7-10 km, which is considerably smaller than expected from hydrostatic equilibrium and thus suggested the action of photochemistry [3]. Imaging observations uncovered two aerosol components: bright, discrete structures at 8 km and mostly poleward of  $30^\circ\text{S}$  (Figure 1), and a global aerosol layer that extends to  $\sim 30 \text{ km}$  at almost everywhere on Triton [71,64].

Voyager 2 revealed the scattering properties of Triton’s aerosols with photometric observations at visible wavelengths (Figure 2). The upturn in the scattered light brightness at large phase angles strongly indicates the presence of reflective aerosols. From the disk-averaged brightness, which

<sup>1</sup> This is also different from its definition in Earth literature.

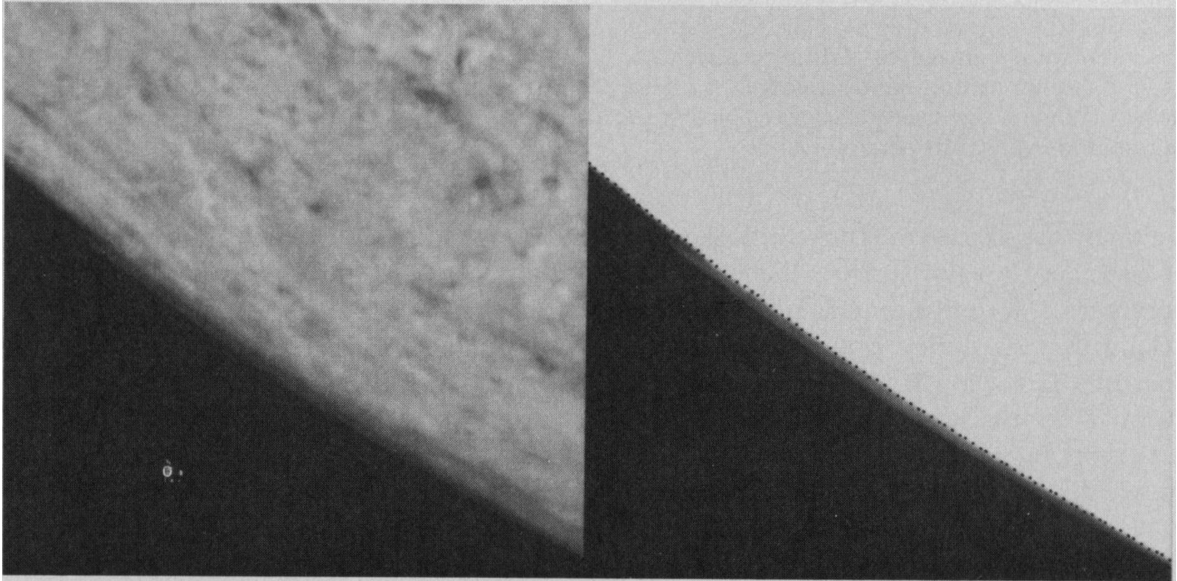


**Fig. 1.** Images of aerosols over Triton's south polar cap taken at the west limb. The left panel highlights the surface features of Triton, while the right panel highlights the limb aerosols, with dark pixels marking Triton's limb. Figure taken from [71].

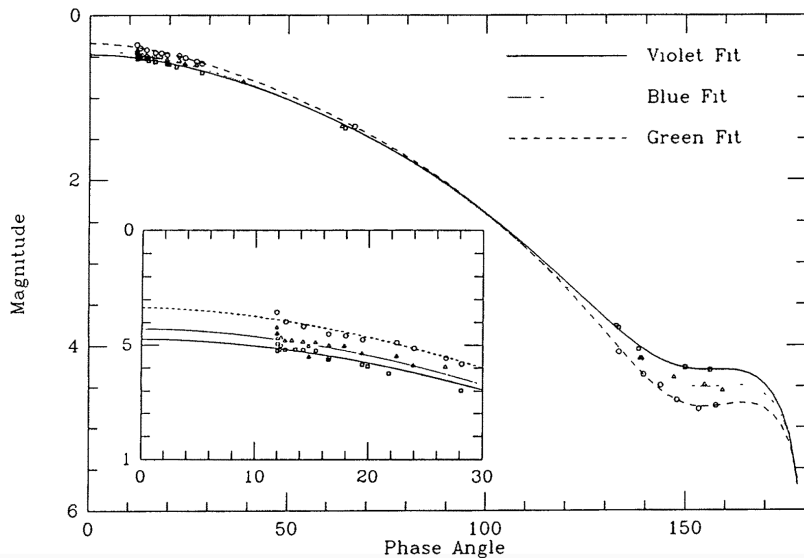


**Fig. 2.** Model phase curves of Triton [29] compared with the Voyager 2 violet, blue, and green filter data. The vertical axis is normalized such that the magnitude at the zero degree phase is  $-2.5 \log(p_{\text{geo}})$ , where  $p_{\text{geo}}$  is the geometric albedo. The disk-averaged image is brighter at smaller phase angles due to surface scattering, while the upturn at large phase angles is due to the scattered light from aerosols. Figure is taken from [29].

predominantly traces the photometric properties of the near-surface discrete structures [30], the vertical aerosol optical depth was constrained to  $\sim 0.03$  at  $\lambda = 0.56 \mu\text{m}$  and followed a wavelength dependence of  $\propto \lambda^{-2}$ , with an asymmetry parameter  $\sim 0.6$  (highly forward scattering) and a single scattering albedo  $\sim 0.99$  [29,28]. However, it should be noted that the single scattering albedo cannot be independently determined apart from the aerosol optical depth for optically thin aerosols.

Spatially-resolved observations help to avoid the ambiguity between the discrete and global aerosol structures when constraining their scattering properties. From spatially-resolved images at high phase angles, the average particle size of the discrete structures at high southern latitudes was constrained

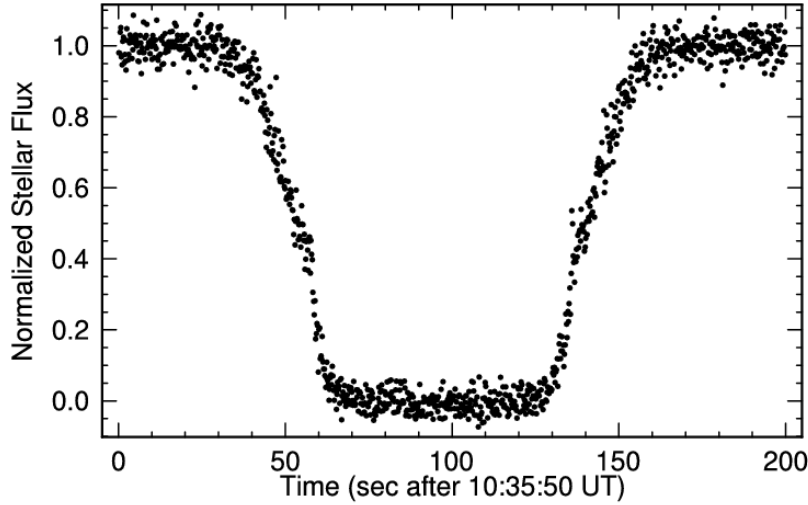


**Fig. 3.** Light curve of the star P8 from the Pluto occultation of 9 June 1988 observed by the Kuiper Airborne Observatory. Figure obtained from [15].

to be  $\sim 0.2\text{--}1.5\ \mu\text{m}$  [64,66]. Meanwhile, at low southern latitudes where the discrete structures are largely absent, the mean particle radius, column-integrated particle number density, and aerosol scale height of the global aerosol layer were estimated to be  $0.17 \pm 0.012\ \mu\text{m}$ ,  $2.0 \pm 0.6 \times 10^6\ \text{cm}^{-2}$ , and  $11 \pm 0.6\ \text{km}$ , respectively, yielding vertical scattering optical depths of  $\sim 0.002\text{--}0.004$  across the visible wavelengths [66]. The fact that the derived scale height was considerably smaller than the pressure scale height at the observed region ( $\sim 16\ \text{km}$ ) suggests that aerosol formation occurred at altitudes below  $20\ \text{km}$ , as the aerosol and pressure scale heights would be identical otherwise.

The vertical extinction profile of Triton’s global aerosol layer was constrained by stellar occultation observations from Voyager 2’s UV spectrometer. The observed extinction at  $0.14\text{--}0.16\ \mu\text{m}$  at altitudes  $< 20\ \text{km}$  had a wavelength dependence suggestive of submicron ( $< 0.3\ \mu\text{m}$ ) particles, as the inferred optical depth at UV wavelengths was orders of magnitude higher than that at visible wavelengths derived from the imaging observations [71,64]. The extinction also differed between ingress and egress [27], while the extinction scale height was identical to the pressure scale height, in contrast to the smaller scale height obtained from spatially-resolved, visible observations [66].

## 2.2 Pre-New Horizons Observations of Pluto’s Atmosphere

Pluto’s atmosphere was detected from groundbased observations of a stellar occultation on 9 June 1988 [33,14,56], which showed a gradual – rather than sudden, in the case of a bare surface – loss of flux from the target star as Pluto occulted it (Figure 3). The “knee” in the light curve at  $\sim 55$  seconds after 10:35:50 UTC, where the stellar flux drops more precipitously, was the first hint that aerosols may pervade the lower atmosphere of Pluto. This is because extinction by aerosols would reduce the stellar flux more quickly than a clear isothermal atmosphere [16]. However, the “knee” can also be explained by a reduction in the atmospheric scale height due to a drastic temperature decrease near the surface [34]. Subsequent stellar occultations from 2002 to 2015, e.g. [13,62,85,63,60,24] found evidence for atmospheric waves and showed that both aerosols and a steep temperature gradient were likely present. Evidence for aerosol extinction was provided by the wavelength-dependence of minimum stellar fluxes consistent with a fall off in aerosol extinction caused by the decrease in absorption of submicron aerosol particles at longer wavelengths [13,24].

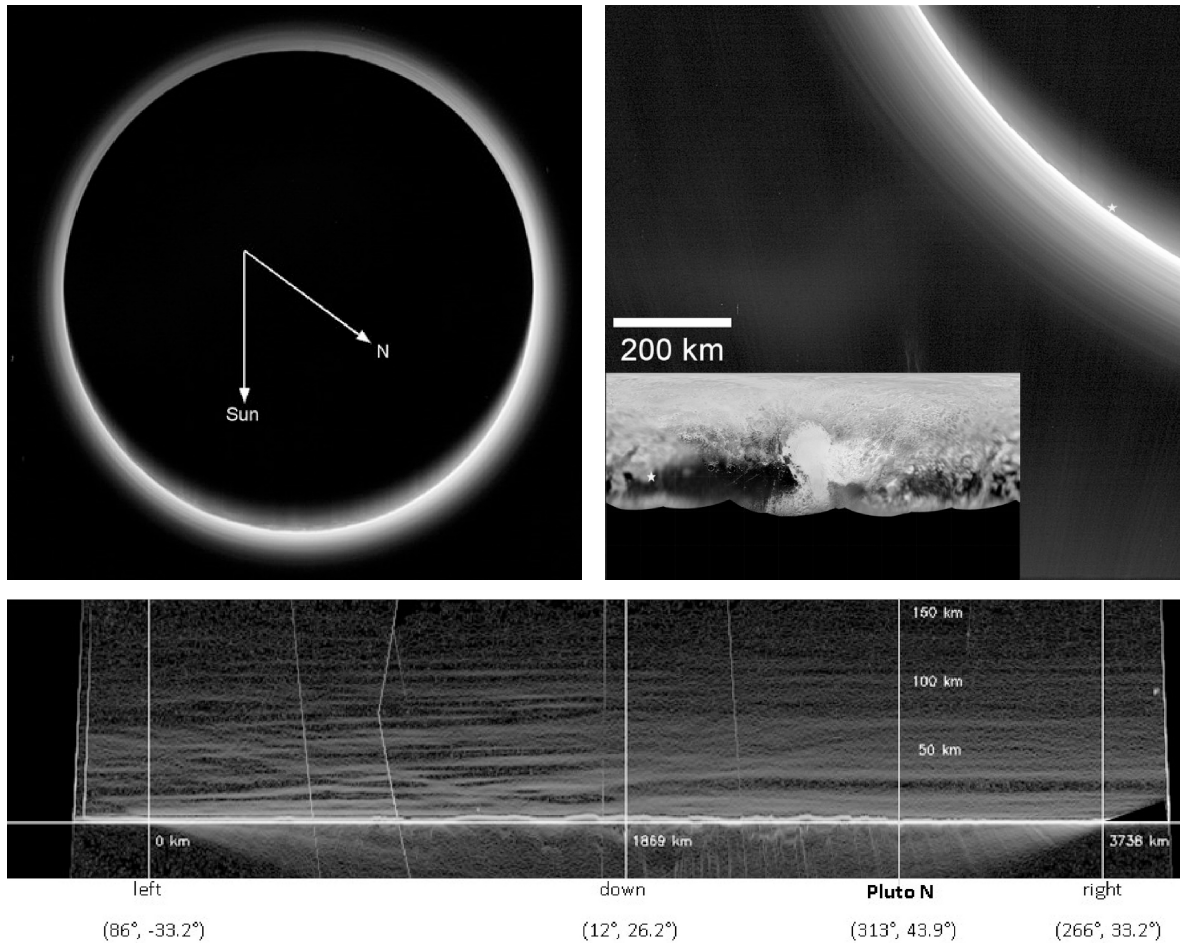


**Fig. 4. Top Left:** New Horizons’s view of Pluto backlit by the Sun, showing the aerosol layers around the full limb. Aerosol scattering is brighter towards the northern (summer) hemisphere rather than the Sun’s direction. Image has been stretched and sharpened. **Top Right:** Close-up of the  $\sim 20$  aerosol layers at Pluto’s limb, with the inset map of Pluto showing the location of the observed aerosols. **Bottom:** Unwrapped mosaic of haze layers around the Pluto limb. Thin, tilted white lines are mosaic seams. Horizontal distance and vertical altitude scales and Pluto longitude/latitude are given. All images are taken by the New Horizons Long Range Reconnaissance Imager (LORRI) and obtained from [6].

The atmospheric composition of Pluto was initially inferred from detections of  $N_2$ ,  $CH_4$ , and CO ices on its surface via infrared spectroscopy [10,61], which implied an atmosphere of similar composition in vapor equilibrium. The finding that  $N_2$  ice was more abundant than the others by a factor of 50, and subsequent measurement of the low surface temperature of Pluto of  $\sim 40$  K [78] all but confirmed  $N_2$  as the dominant atmospheric gas due to its volatility. Direct detections of gaseous  $CH_4$  and CO were subsequently made through high resolution spectroscopy [87,50].

### 2.3 New Horizons Observations of Pluto Aerosols

The New Horizons spacecraft flew through the Pluto system on 14 July 2015 and confirmed the existence of aerosols in Pluto’s atmosphere (Figure 4). The aerosols were found to be optically thin but global, with nadir optical depths of  $\sim 0.01$  at optical wavelengths but wrapping around the full limb [22]. Unlike Triton, no discrete aerosol structures were detected conclusively [73]. Aerosol scattering was brighter towards the northern (summer) hemisphere by a factor of 2 to 3 compared to equatorial regions, suggesting a factor of 2 greater aerosol mass loading. Aerosol scattering at optical wavelengths was observed to 200 km altitude above the surface, while UV extinction by aerosols was seen reaching

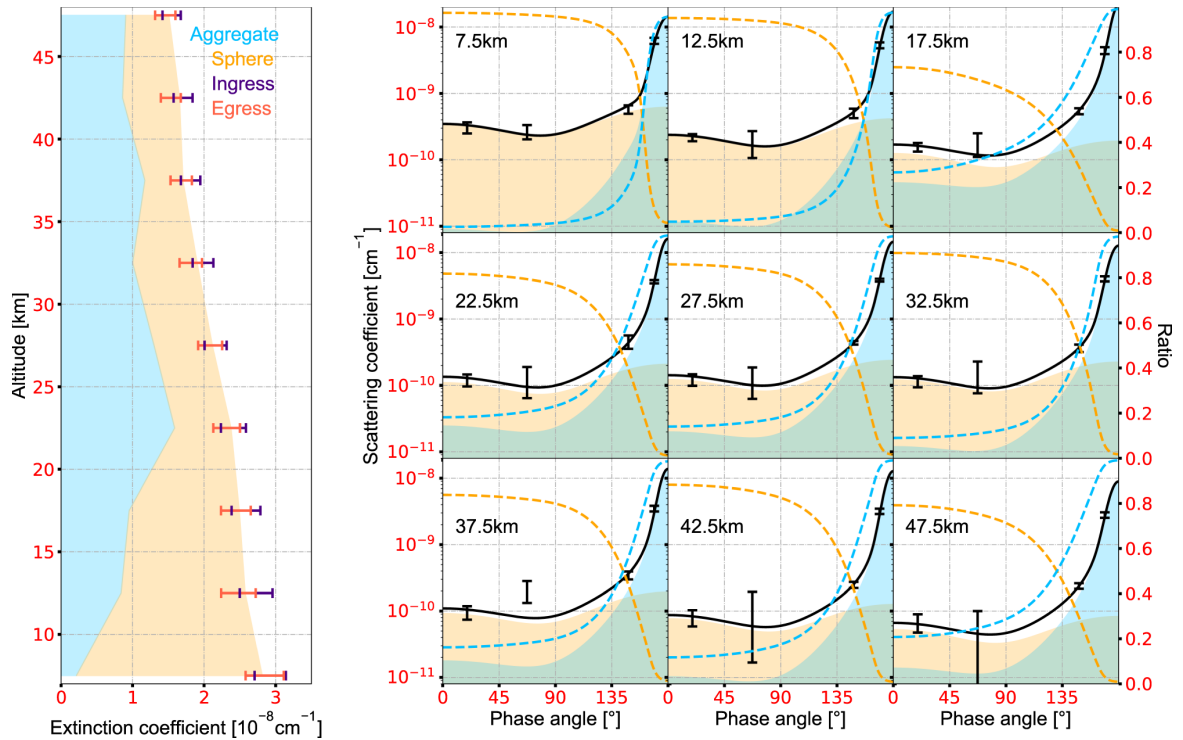


**Fig. 5.** **Left:** Near-surface aerosol extinction at Pluto observed by the Alice spectrograph during ingress (indigo) and egress (red) of solar occultation compared to the modeled contributions from large  $\sim 1 \mu\text{m}$  aggregates (blue) and smaller particles of a few tens of nm radius (orange). **Right:** Near-surface scattered light observations obtained by LORRI (black) compared to the modeled contributions from large aggregates and small particles. Black curves denote the total contributions of aggregates and spheres. Colored dashed curves represent the ratio of contribution from each component. Figures taken from [17].

500 km. The vertical distribution of aerosols was not smooth, but consisted of  $\sim 20$  fine distinct layers each with a thickness of a few km separated on average by about 10 km, though in general aerosol scattering increased with decreasing altitude. Contrast between the bright layers and the darker regions in between is a few percent. Each thin aerosol layer was observed to extend for hundreds of km around the limb, and sometimes merging with others or splitting apart [6,35]. Pluto’s aerosols appear to be more Titan-like and absorbing than Triton’s, with single scattering albedo ranging from 0.9-0.95 over wavelengths of 500 to 900 nm [31].

The wavelength and phase angle dependence of aerosol extinction point to a complex aerosol particle distribution (Figure 5). The aerosol scattering intensity in the visible and near-IR showed a gradual decrease with increasing wavelength, suggesting aerosol particle sizes of  $\sim 10 \text{ nm}$  [22,23,44]. However, the aerosols were also found to be highly forward scattering in the visible, which is indicative of larger ( $>0.1 \mu\text{m}$ ) particles. Furthermore, the ultraviolet aerosol extinction indicated a large aerosol UV cross section that cannot be produced by even  $0.1 \mu\text{m}$  spherical particles [88,39]. Porous fractal aggregates – irregularly shaped, extended particles composed of loosely bound, small, roughly spherical monomers (see §3.2) – provide a possible explanation for these seemingly conflicting observations [82]: the wavelength dependence and large UV cross section are due to scattering and extinction by the collection of  $\sim 10 \text{ nm}$  monomers, while the forward scattering is accomplished by the large ( $>0.1 \mu\text{m}$ ) extended nature of the particles [6]. However, while fractal aggregate particles fit the observations at altitudes above 50 km, an increase in the aerosol backscattering intensity near the surface cannot be reproduced by this population alone. Here, two separate populations of aerosol particles are required: smaller particles (spherical or aggregate) with radii of a few tens of nm that are capable of producing the observed backscattering, and  $\sim 1 \mu\text{m}$  fractal aggregates with  $\sim 10 \text{ nm}$  monomers that can explain the large forward scattering and UV extinction and wavelength dependence (Figure 5) [44,17].

The abundance profiles of several key gases in Pluto’s atmosphere were constrained through solar and stellar UV occultations observed by the New Horizons Alice UV spectrograph [88,39]. N<sub>2</sub> and CH<sub>4</sub> were shown to be the dominant gases in the atmosphere, with mixing ratios of 99% and 1% near the surface, respectively. Diffusive separation at high altitudes results in the mixing ratio of CH<sub>4</sub> approaching 5% at ~500 km. C<sub>2</sub>H<sub>2</sub>, C<sub>2</sub>H<sub>4</sub>, and C<sub>2</sub>H<sub>6</sub> were also identified, which are likely photochemical in origin (see §3.1). Interestingly, these species are not well-mixed in the atmosphere below their nominal photochemical production altitude, and instead show depletion below 400 km suggestive of chemical destruction and/or condensation. The mixing ratio profile of HCN, which was measured by ALMA at nearly the same time as the New Horizons flyby, shows similar decreases below 400 km, but also a highly supersaturated mixing ratio in the upper atmosphere [51].

## 2.4 Summary

Observations of Triton and Pluto’s atmospheres show that both worlds possess global aerosol layers with intriguing differences and similarities. The biggest difference is the vertical extent of the aerosols: while Triton’s aerosols are confined to the lower ~30 km of the atmosphere, Pluto’s extend to >500 km. In addition, Triton possesses two distinct aerosol populations: a low optical depth global layer and higher optical depth near-surface discrete structures. In contrast, Pluto lacks discrete structures (though there are extensive vertical layering, which is not present on Triton), but still appears to possess two particle populations near the surface, with particle sizes similar to the two Triton aerosol populations. The total vertical optical depths of the aerosols on both worlds are also strikingly similar at around 0.01, though Triton’s is more variable due to the discrete structures.

## 3 Theory of Triton and Pluto Aerosols

### 3.1 Photochemistry and Aerosol Formation on Triton and Pluto

The origins of aerosols in the cold reducing atmospheres of Triton and Pluto are inexorably tied to the photochemistry of N<sub>2</sub> and CH<sub>4</sub>. N<sub>2</sub> is destroyed by extreme-UV (EUV) solar photons ( $\lambda < 100$  nm) and, additionally for Triton, high energy electrons from Neptune’s magnetosphere [53,91,45]; CH<sub>4</sub> is photolyzed mostly by Lyman- $\alpha$  photons from the Sun and those scattered by the local interstellar medium [75,45]. These reactions yield radical species such as N, H, CH, <sup>3</sup>CH<sub>2</sub>, and CH<sub>3</sub>, which rapidly react with each other to form more complex hydrocarbons and nitriles like C<sub>2</sub>H<sub>2</sub>, C<sub>2</sub>H<sub>4</sub>, C<sub>2</sub>H<sub>6</sub>, C<sub>4</sub>H<sub>2</sub>, and HCN [75,43,45,84,52,1].

A key difference in the photochemistry of Triton and Pluto is the near-surface gaseous CH<sub>4</sub> abundance, which is a factor of 10-100 smaller on the former compared to the latter. This results in CH<sub>4</sub> being photolyzed, and thus more complex hydrocarbons and nitriles being produced, at a much lower altitude on Triton – at around 25 km [41] – in contrast to 400 km on Pluto [45,84,42]. The rapid destruction of CH<sub>4</sub> near the surface of Triton explains the observed small CH<sub>4</sub> scale height of 7-10 km and the lack of CH<sub>4</sub> at higher altitudes [3]. In contrast, the abundant CH<sub>4</sub> on Pluto overwhelms any photochemical destruction, allowing it to persist into the upper atmosphere (Figure 6) [41,86].

Lessons learned from the analysis, modeling, and experimental interpretation of Cassini observations of Saturn’s moon, Titan, can be applied to understand the connection between photochemistry and haze formation on Triton and Pluto. All three bodies possess N<sub>2</sub>-dominated atmospheres with trace amounts of CH<sub>4</sub>, though Titan’s atmosphere is significantly more massive. Similar to Triton and Pluto, N<sub>2</sub> and CH<sub>4</sub> are destroyed in the upper atmosphere and ionosphere of Titan (~1000 km altitude) through photolysis by EUV and FUV (far-UV) photons and energetic particles from Saturn’s magnetosphere [67,20], producing radicals and progressively more complex organic molecules and ions, e.g. [90,83,81]. Cassini observations show that this process of atmospheric species gradually increasing in complexity and mass through successive neutral and ion reactions continues smoothly up to heavy negative ions with masses of ~10<sup>4</sup> Da q<sup>-1</sup> [7,80]. These negative ions attract the less massive (up to 350 Da q<sup>-1</sup> [9]) positive ions in Titan’s ionosphere and grow rapidly as a result, eventually forming the nm-sized “seeds” of Titan’s global hazes [48].

The complex chemistry and formation of hazes on Titan depends heavily on the coupling between neutral and ion chemistry in its ionosphere. Titan’s ionosphere exhibits an electron density peaking

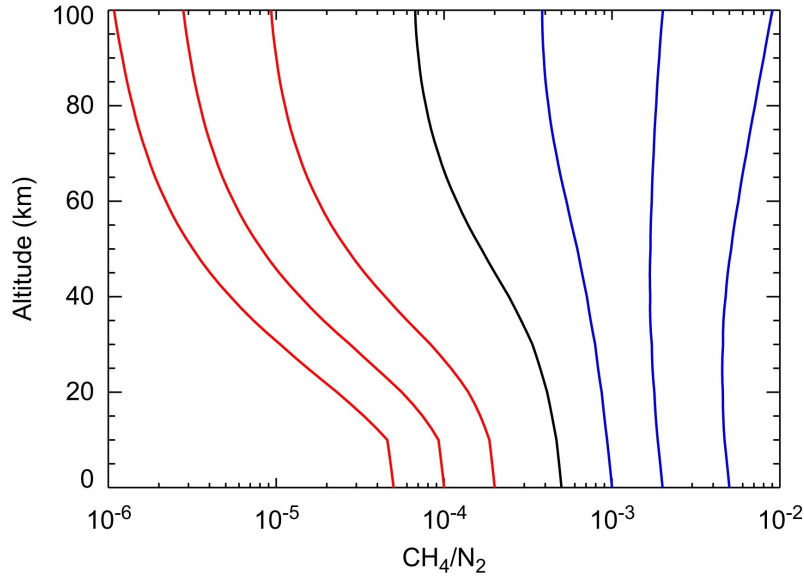


**Fig. 6.** CH<sub>4</sub> mixing ratio profiles on Triton as functions of its value near the surface. Photolysis and chemical reactions tend to reduce methane (red) while diffusive separation enhances it (blue). Transition between the two regimes (black) occur at a surface CH<sub>4</sub> mixing ratio of  $\sim 5 \times 10^{-4}$ . Figure taken from [41].

at  $\sim 3000 \text{ e}^- \text{ cm}^{-3}$  [67] and a smorgasbord of organic molecules and ions sourced from N<sub>2</sub> and CH<sub>4</sub>. In comparison, New Horizons only placed an upper limit of  $1000 \text{ e}^- \text{ cm}^{-3}$  on Pluto’s ionosphere, which is otherwise populated by positive molecular ions [32]. Triton’s ionosphere exhibits an even greater electron density than Titan of  $25000\text{-}45000 \text{ e}^- \text{ cm}^{-3}$  [79] due to the lack of CH<sub>4</sub> allowing the survival of atomic species and ions [43], which in turn possess long enough lifetimes to ensure high electron densities [74]. However, the low abundance of CH<sub>4</sub> at high altitudes also makes complex organic chemistry difficult. In addition, the atmospheres of Triton and Pluto both contain about 10 times the abundance of CO as Titan (500 ppm vs. 50 ppm) [25,49,51]. These differences could result in significant disparities in the haze properties of these atmospheres.

### 3.2 Formation, Evolution, and Dynamics of Triton and Pluto Aerosols

The size and spatial distributions of aerosols are controlled by transport processes such as sedimentation, diffusion, and advection, as well as microphysical processes including nucleation, growth through condensation and coagulation, and loss through evaporation/sublimation. In the following sections, we summarize several key microphysical processes relevant to Triton and Pluto aerosols and what models that consider these processes have shown.

**Haze Particle Transport** Upon formation, nm-sized nascent haze particles will begin settling downwards at their terminal velocities due to gravity. At the low gas densities of Pluto and Triton’s atmosphere, the mean free path of gas molecules is much larger than the haze particle radii (large Knudsen number), so that particle transport occurs in the gas kinetic regime. As a result, the terminal velocity is linearly proportional to the particle mass density and radius (for compact particles) and inversely proportional to the ambient gas density.

In addition to sedimentation, aerosol particles are also transported by atmospheric circulation. Unfortunately, only one study [2] has investigated the impact of circulation on Pluto’s hazes, and none have focused on similar processes on Triton. [2] simulated the formation, sedimentation, and horizontal advection of haze particles at the time of the New Horizons flyby and showed that the haze distribution is strongly tied to whether N<sub>2</sub> is condensing out on the (unobserved) south pole. Without N<sub>2</sub> condensation, the meridional flow is weak and hazes do not experience significant horizontal transport, resulting in a concentration of hazes in the northern (summer) hemisphere where the Lyman- $\alpha$

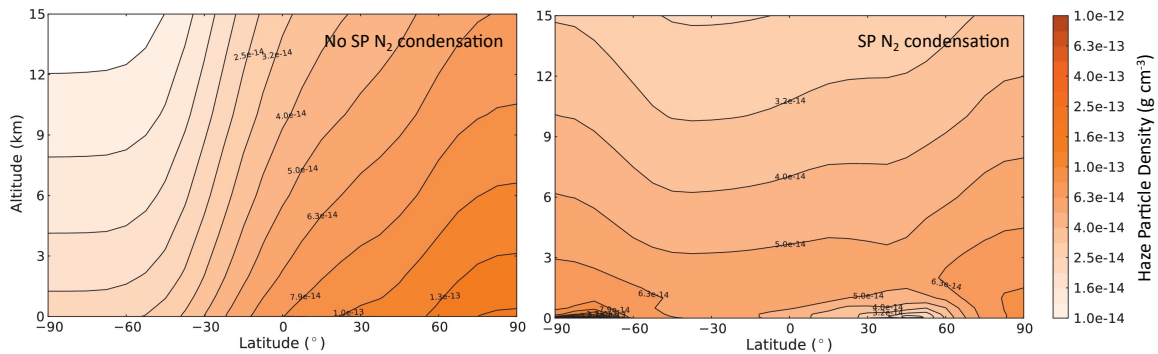


**Fig. 7.** Zonal mean Pluto haze particle density without (left) and with (right)  $N_2$  condensation at the south pole, as computed by a 3D model. Figure taken from [2].

flux is the highest. In contrast,  $N_2$  condensation strengthens north-to-south meridional winds due to conveyance of  $N_2$  from Sputnik Planitia to the south pole, resulting in a more homogeneous haze latitudinal distribution. Hazes would also be depleted near the surface over Sputnik Planitia due to the upward branch of the flow, and enriched over the south pole due to the downward branch (Figure 7). Current observations cannot discriminate between these two scenarios [6,5].

The observed layering of hazes in Pluto’s atmosphere [22,6,35] may be caused by atmospheric waves, which have been observed as temperature perturbations during groundbased stellar occultations, e.g. [62,85,63]. These waves could be caused by thermal tides arising from  $N_2$  sublimation [77,19] and/or gravity waves arising from orographic forcing [22,6]. Such waves could act to compactify and rarefy haze distributions, generating the observed layers. However, neither explanation is perfect: the thermal tide hypothesis does not explain how haze particles are transported by the waves and assumes zero mean flow while the orographic forcing hypothesis involves topography that may be too localized to explain the global haze layers [35]. Follow up work is needed to model these processes more rigorously.

**Haze Particle Growth** Haze particles can grow as they are transported in the atmosphere. The primary pathway for growth of involatile haze particles is coagulation, when particles collide and stick together. For the submicron particles observed in Pluto’s and Triton’s atmospheres, thermal Brownian motion is the main driver of relative velocities and collisions. While it is typically assumed that every particle collision leads to sticking, microphysical studies of Titan’s hazes have shown that haze particle charging via interactions with ions and electrons may prevent sticking, thereby regulating the coagulation rate and haze particle size distribution e.g. [47]. The impact of particle charge is typically parameterized by a charge-to-radius ratio.

Growth of haze particles via coagulation can lead to non-spherical particle shapes, which drastically alters their aerodynamical and optical properties. Non-spherical haze particles have typically been treated as fractal aggregates composed of smaller spherical monomers. The shape of a fractal aggregate is characterized by the fractal dimension  $D_f$ , which is related to the number of monomers in an aggregate  $N_{\text{mon}}$ , monomer radius  $r_{\text{mon}}$ , and aggregate characteristic radius  $r_{\text{agg}}$  (the radius of a sphere that has the same gyration radius) via

$$N_{\text{mon}} = k_0 \left( \frac{r_{\text{agg}}}{r_{\text{mon}}} \right)^{D_f}, \quad (1)$$

where  $k_0$  is an order unity prefactor. Particles with  $D_f = 1$  are chain-like aggregates, while a  $D_f = 2$  particle possesses a mass that is proportional to its cross sectional area. Equation (1) indicates that the internal density of aggregates decreases with addition of monomers, while the terminal velocity of the aggregate is the same as that of its monomers when  $D_f \sim 2$ , which is typical of aggregate formation via ballistic cluster-cluster collisions [4].

Haze microphysical models of Pluto and Triton typically simulate the vertical transport and growth (by coagulation) of haze particles initially produced at the pressure level of  $\text{CH}_4$  photolysis, with the production rate as a free parameter. For Pluto, microphysical models typically require haze production rates on par with the methane photolysis rate due to solar and local interstellar medium-scattered UV (a few times  $10^{-14} \text{ g cm}^{-2} \text{ s}^{-1}$ ) to match the observed stellar occultation light curves [72] and UV extinction from New Horizons [21]. The latter study also found that aggregate particles with 10 nm monomers and  $D_f = 2$ , similar to haze particles on Titan [70], are preferred over compact spherical particles (Figure 8). [21] further found that reproducing the inferred near-surface particle size of  $\sim 0.1 \mu\text{m}$  observed by LORRI [22] necessitated particle charging, with a charge-to-radius ratio of  $\sim 30 \text{ e}^- \mu\text{m}^{-1}$ , about twice that of Titan [47]. However, subsequent comparisons of the models of [21] to MVIC data suggested a higher value of  $\sim 60 \text{ e}^- \mu\text{m}^{-1}$  [44]. For Triton, similar modeling has been conducted by [59], who in addition explicitly simulated the evolution of aggregate volume through different-sized aggregate collisions in each mass bin. They found that haze particles on Triton can grow into aggregates with  $D_f \sim 1.8\text{--}2.2$ , though the available observations are insufficient for constraining the actual fractal dimension of Triton aerosols and their charge-to-radius ratios. Critically, [59] found that hazes could not simultaneously explain both the observed UV extinction coefficient and visible scattered-light intensity due to absorption by the haze, and that brighter material, such as hydrocarbon ices, must be present.

**Cloud Formation** The low temperatures of Triton’s and Pluto’s atmospheres likely lead to ice cloud formation. Cloud particles form through nucleation, when gas molecules cluster together freely (homogeneous nucleation) or around a cloud condensation nucleus (CCN; heterogeneous nucleation) to form a volatile particle. In the latter case, the CCN is typically another type of particle in the atmosphere. The nucleation rate is dependent on the saturation vapor pressure and the material properties of the condensate, including its surface energy and molecular weight; in the case of heterogeneous nucleation, the rate also depends on the number density, size, and material properties of the CCN, in particular the desorption energy of condensate molecules on the CCN surface and the contact angle between the condensate and the CCN. In general, high surface energies and mean molecular weights, low CCN number densities, small CCN sizes, low desorption energies, and large contact angles lead to lower nucleation rates for a fixed temperature and condensate vapor supersaturation [65]. The inclusion of charged particles can increase the nucleation rate through the introduction of electric potential energy, lowering the energy barrier to nucleation [58].

Following nucleation, cloud particles can grow through condensation. In the gas kinetics regime, the condensation rate depends on the abundance and thermal velocity of the condensate vapor, as well as the cloud particle size through the Kelvin curvature effect. The Kelvin effect is the increase in the saturation vapor pressure over a curved surface as compared to that over a flat surface owing to the weaker binding energy of molecules on the former [65]. As such, smaller particles tend to grow slower and evaporate faster.

Ice clouds as an explanation for the aerosol structures on Triton was a popular hypothesis following the Voyager 2 encounter, owing to their high albedo and supporting evidence from photochemical models [71,75,64,28,66,74]. In particular, [75,74,43] showed that  $\text{CH}_4$  photolysis yielded sufficient  $\text{C}_2$  hydrocarbons that condensed out in the lower 30 km of Triton’s atmosphere (column production rate of  $\sim 4 - 8 \times 10^{-15} \text{ g cm}^{-2} \text{ s}^{-1}$ ) to match the observed optical depth of the global aerosol structure. Meanwhile, the discrete aerosol structures below  $\sim 8$  km were assumed to be  $\text{N}_2$  ice clouds, as they were mostly detected over the southern  $\text{N}_2$  polar cap where they could form through large scale upwelling from surface  $\text{N}_2$  sublimation and/or plume activity, with  $\text{N}_2$  vapor possibly nucleating on the  $\text{C}_2$  hydrocarbon ice particles [64,66]. More recently, [59] considered condensation of  $\text{C}_2\text{H}_4$  onto haze CCN and found that the resulting ice cloud could explain both the observed UV extinction coefficient and visible scattered-light intensity assuming a  $\text{C}_2\text{H}_4$  production rate consistent with the photochemical production rate of higher order hydrocarbons computed by [75] (Figure 8). The ice cloud is present primarily below 30 km, matching the vertical distribution of Triton’s global aerosol layer. Under this scenario, haze CCN is produced at  $>250$  km with a rate of only  $6 \times 10^{-17} \text{ g cm}^{-2} \text{ s}^{-1}$ , resulting in little observable haze above 30 km. These results were corroborated by [46], who further found

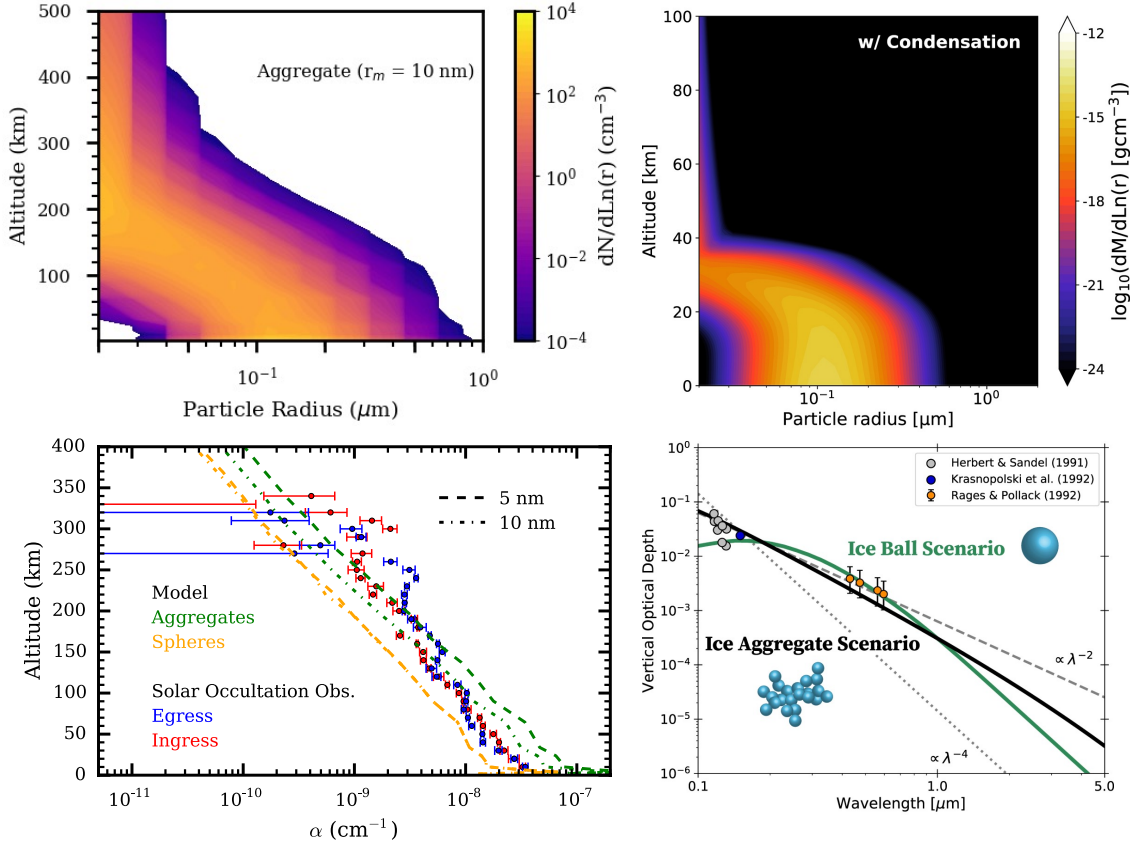


**Fig. 8.** Number densities of aerosol particles as a function of altitude and particle radius for Pluto hazes, assuming aggregates with 10 nm monomers (top left) and Triton hazes and ice clouds (top right) from the microphysical models of [21] and [59], respectively. **Bottom left:** Comparison of extinction coefficient  $\alpha$  of spherical (orange) and aggregate (green) haze particles with 5 nm (dashed) and 10 nm monomers (dash dot; the 10 nm aggregate model is the same as that presented in the top left panel) with the observed ingress (red) and egress (blue) solar occultation observations at Pluto [22]. **Bottom right:** Comparison of the vertical optical depth of the ice balls (green line; same model as that plotted top right) and ice aggregates (black line) models for Triton aerosols with the observed optical depths from [27] (gray), [40] (blue), and [66] (orange). All figures taken from [21] and [59].

through tracking the evolution of  $D_f$  from relative contributions of ice condensation and coagulation that  $D_f = 3$  above 50 km and transitions to 2 below 25 km as coagulation becomes more important.

Ice cloud nucleation onto haze CCN in Pluto’s middle atmosphere may explain the depletion of gaseous HCN and C<sub>2</sub>-hydrocarbons below 400 km. Using a photochemical model, [84] showed that the shapes of their observed mixing ratio profiles can be reproduced if they condensed onto haze CCN, though the C<sub>2</sub>H<sub>4</sub> saturation vapor pressure may need to be lower than that extrapolated from laboratory measurements, or else atmospheric mixing may need to be stronger and/or ion chemistry may need to be considered [42]. In contrast, [52,54] considered adsorption of gas molecules on haze particles and found similar magnitudes of gas depletion. Adsorption is more dependent on the surface chemistry of haze particles than saturation vapor pressures, with [52] finding that Pluto’s hazes must become less “sticky” to gas molecules as they age due to chemical evolution, which is similar to what is seen for Titan’s hazes [12]. [46] also found that adsorption of C<sub>2</sub>-hydrocarbons is possible, but on ice clouds made of HCN, C<sub>3</sub>H<sub>4</sub>, C<sub>4</sub>H<sub>2</sub>, and C<sub>6</sub>H<sub>6</sub> instead of haze CCN, as they found condensation of these ices to be abundant in their model below 400 km. [46] further found that ice clouds could make up a significant fraction of the mass of Pluto aerosols, and that  $D_f = 3$  above 400 km and 2 below 300 km, with a smooth transition in between as sedimenting spherical particles coagulate into aggregates.

Gas condensation also impacts Pluto’s upper and near-surface atmosphere. At high altitudes where haze CCN is absent, nucleation rates of ice particles may be extremely slow [69], potentially explaining the large ( $>10^6$ ) HCN supersaturation observed by ALMA [51]<sup>2</sup>. Meanwhile, [73] simulated the condensation of hydrocarbon and nitrile ice clouds within 15 km of Pluto’s surface where temperatures reach 40 K and found relatively low cloud optical depths ( $\tau \sim 10^{-4}$ ), though small ( $\sim 1 \text{ m s}^{-1}$ ) updrafts could promote much more optically thick ( $\tau \sim 0.1$ ) clouds. Such cloud formation could lead to a sharp increase in  $D_f$ , as shown by [46]. It should be noted, however, that the microphysical parameters used in all of the aforementioned studies, such as the saturation vapor pressure, surface energy, and contact angles between the condensing gases and haze CCN are largely unknown and/or uncertain due to a lack of laboratory measurements at the relevant temperatures.

### 3.3 Summary

The photochemical destruction of  $\text{N}_2$  and  $\text{CH}_4$  in Triton’s and Pluto’s atmospheres likely serves as the origins of the clouds and hazes therein. Such photochemical processes produce an array of simple hydrocarbon and nitrile molecules that can react further to form massive charged ions and nm-sized organic haze particles. Alternatively, the simple molecules can condense out and form highly reflective ice clouds that likely nucleate on haze CCN. Models of Triton’s and Pluto’s aerosols predict that the differences in the aerosol composition and distributions of the two bodies are likely caused by the gaseous methane abundance near their surfaces: the relatively high abundance of methane in Pluto’s atmosphere allows methane to survive to hundreds of km altitude, where its photolysis leads to the formation of complex haze particles; in contrast, the lower abundance of methane in Triton’s atmosphere results in its photolysis within a few tens of km of its surface, leading to the production of hydrocarbon molecules that condense to form ice clouds. In both Triton and Pluto’s atmospheres, aerosol particles sediment from their source towards the surface, with little impact from diffusional processes, though global circulation may be important on Pluto. Both spherical and fractal aggregate particles are likely present, and they may transition from one form to another depending on whether condensation or coagulation is dominant. Finally, it is uncertain whether condensation or sticking/adsorption is more important in Pluto’s atmosphere due to uncertainties surrounding the microphysical parameters of the relevant gaseous and CCN species such as their saturation vapor pressures and surface energies.

## 4 Laboratory Investigations of Triton and Pluto Aerosols

Laboratory experiments are essential for constraining the material and optical properties of aerosols necessary for modeling aerosol formation and evolution and interpreting observations. To this end, a number of studies have attempted to synthesize photochemical haze analogs by subjecting gas mixtures replicating the compositions of Pluto’s and Triton’s atmospheres to an energy source. For example, both [76] and [55] analyzed Triton haze analogs produced from exposing a  $\text{N}_2/\text{CH}_4(0.1\%)$  gas mixture to cold plasma and found remarkable differences in their C/N ratio and spectral features compared to Titan haze analogs, indicating that differences in  $\text{N}_2/\text{CH}_4$  ratios led to different reaction pathways in haze production, and that electrons coming from Neptune’s magnetosphere likely promote the production of absorbing organic hazes. More recently, [57] performed a cold plasma experiment on a  $\text{N}_2/\text{CH}_4(0.2\%)/\text{CO}(0.5\%)$  gas mixture at 90 K and found that the addition of CO results in nitrogen-rich (rather than carbon-rich) Triton haze analogs that incorporate oxygen at  $\sim 10 \text{ wt}\%$ , indicating that the relative abundance of CO also plays key roles in controlling the properties of organic hazes. Meanwhile, [38,37] investigated the altitude dependence of haze composition on Pluto by considering a  $\text{N}_2/\text{CH}_4/\text{CO}$  gas mixture where the CO abundance is fixed to 500 ppm and the  $\text{CH}_4$  abundance is allowed to vary from 0.5 to 5% to simulate high altitude diffusive separation. They found that more N and O atoms were incorporated in the sample with lower  $\text{CH}_4$  abundances, showing that haze composition likely varies with altitude. They also found that the Pluto haze analogs were less

<sup>2</sup> In comparison, supersaturation of water vapor on Earth almost never exceeds a few % due to the ample abundance of CCN [65].

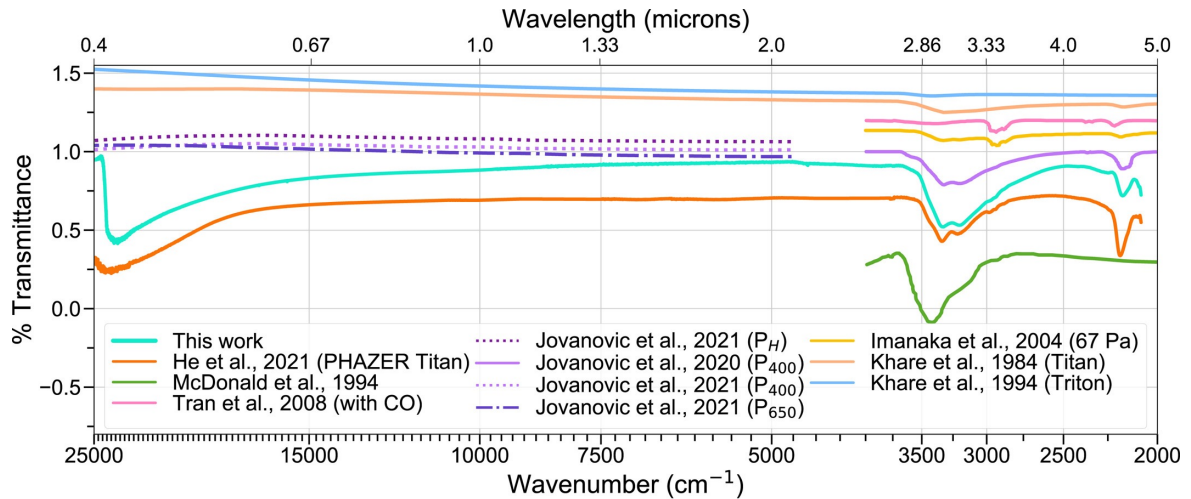


**Fig. 9.** Transmittance spectra of organic haze analogs produced in laboratory experiments from mixtures of  $N_2$  and  $CH_4$  (and CO in some cases) replicating the atmospheres of Titan (orange, pink, yellow, and salmon), Pluto (light/dark purple dotted and dash-dot), and Triton (cyan, green, and light blue). See Table 3 of [57] for details on the individual studies. Figure taken from [57] (“This work” in the figure).

absorbing at optical wavelengths compared to Titan haze analogs, which are produced without CO gas (Figure 9). Finally, [26] considered a  $N_2/CH_4/CO$  gas mixture with varying CO abundances that is applicable to Titan, Triton, and Pluto, and found an increase in the density and oxygen content and a decrease in the saturation of the haze analogs with increasing CO.

To aid our understanding of ice cloud formation in Triton’s and Pluto’s atmosphere, several studies have measured and compiled the saturation vapor pressures and surface energies of relevant hydrocarbon and nitrile ices [58,18,89]. However, the temperature ranges for which the measurements are valid often do not contain the low temperatures of Triton and Pluto, and thus caution is required when extrapolating the empirical saturation vapor pressure and surface energy expressions. Measurements of other microphysical parameters, such as the desorption energies and contact angles between condensates and CCN are relatively rare, and confined mostly to methane and ethane condensates and haze CCN [11,68].

## 5 Triton and Pluto Aerosols: Unknowns and Outlook

Despite similarities in atmospheric composition and surface pressures and temperatures, the aerosols of Triton and Pluto are distinct from each other (Table 1). Triton hosts a global aerosol layer likely composed of organic ices that is confined to the lower few tens of km of its atmosphere, with discrete clouds below 10 km, while Pluto’s aerosols are seemingly dominated by organic hazes extending up hundreds of km with multiple fine layers, though organic ice adsorption and/or condensation also likely play a role. This difference has been hypothesized as being driven by the difference in  $CH_4$  abundance on the two worlds: the lower  $CH_4$  abundance on Triton leads to  $CH_4$  and  $N_2$  photochemistry in the lower few tens of km, leading to production and condensation of simple hydrocarbon and nitrile ices. Meanwhile, the higher  $CH_4$  abundance on Pluto allows it to survive into the upper atmosphere, resulting in the production of organic haze particles at hundreds of km altitude from a rich network of neutral and ion reactions; these particles then sediment downwards and could act as nucleation centers and/or adsorbing surfaces for gaseous hydrocarbon and nitrile species.

Groundbased stellar occultations, the Voyager 2 and New Horizon flybys, and lessons learned from Cassini observations of Titan have increased our knowledge of Triton’s and Pluto’s aerosols considerably, but many vital unknowns remain. Due to the limitations in wavelength and phase angle of the existing observations, the composition, and therefore formation mechanism of Triton’s and Pluto’s aerosols remain uncertain. While parallels could be drawn between the organic hazes and ice clouds

**Table 1.** Summary of Triton and Pluto aerosol properties. See §2 and §3 for details.

	Triton	Pluto
Spatial distribution	global + discrete structures, up to 30 km [71,64]	global, layered, up to 500 km [22]
Production rate	$2\text{--}8 \times 10^{-15} \text{ g cm}^{-2} \text{ s}^{-1}$ [59]	$\sim 10^{-14} \text{ g cm}^{-2} \text{ s}^{-1}$ [21]
Composition	N <sub>2</sub> ice (discrete) [64] organic ices (global) [59,46]	organic haze + ices [21,46]
Size	$\sim 0.2\text{--}1.5 \mu\text{m}$ (discrete), [64,66] $\sim 0.15 \mu\text{m}$ (global) [40,66]	$\sim 0.1\text{--}1 \mu\text{m}$ [17]
Shape	unconstrained [59]	spheres + aggregates [17]
Charge	unconstrained [59]	$30\text{--}60 \text{ e}^- \mu\text{m}^{-1}$ [21,44]
Optical depth	$\sim 0.03$ (discrete), [64] $\sim 0.003$ (global) [66]	$\sim 0.01$ [22]
Single scattering albedo	0.99 [29,28]	0.9-0.95 [31]

of Titan and those on Triton and Pluto, the different atmospheric compositions (i.e. higher CO on the latter bodies), energy sources, and ionospheric environments could result in significant differences in the formation and evolution of the aerosols of the three worlds. In addition, the impact of aerosols on the atmospheric radiative transfer and dynamics of Triton and Pluto requires further study. For example, [92] explained the observed low escape rate of Pluto’s atmosphere by showing that Pluto’s aerosols could significantly cool its upper atmosphere. This would indicate a fundamental connection between atmospheric and surface volatile evolution, photochemistry, and aerosol formation in Pluto’s atmosphere that is likely modulated by Pluto’s extensive seasonal cycles caused by its eccentric orbit [36]. Similar connections between Triton’s aerosols and the rest of Triton’s atmosphere may also exist and therefore should be investigated.

Furthering our understanding of Triton’s and Pluto’s aerosols requires synergy between observations, modeling, and laboratory studies. A dedicated orbiter at Triton and/or Pluto would greatly increase our knowledge of their aerosols by observing their atmospheres at a wide range of phase angles and wavelengths, and by monitoring them for temporal and spatial variations in aerosol distributions and optical properties. In particular, spectral features associated with solid organic material are abundant at longer, mid-infrared wavelengths [92]. Meanwhile, laboratory measurements of key microphysical parameters at Triton and Pluto temperatures, such as the saturation vapor pressure, surface energy, desorption energy, and contact angles of organic ices and haze analogs would be essential for more accurate modeling of ice cloud formation and how hydrocarbon and nitrile species interact with organic haze particles. Further laboratory work on haze formation is also needed, particularly in how they initially form from gaseous species and how they grow through condensation and/or coagulation into spheres or aggregates. In addition, uncertainties in the aerosols’ optical properties remain a major bottleneck in interpreting observations and thus more measurements are needed. At the same time, modeling efforts that take into account the laboratory measurements and additionally focus on how hazes interact with the 3D radiative environment and dynamics of the atmosphere, along with how they evolve on seasonal timescales would also greatly aid in understanding current and future observations. Finally, given that the differences between Triton’s and Pluto’s aerosols likely hinge on the surface CH<sub>4</sub> abundance, observing and modeling these surfaces and the near-surface atmosphere through time would help us better understand whether Triton’s and Pluto’s aerosols are fundamentally different or they are simply different points on the same evolutionary path.

## References

1. B. Benne, M. Dobrijevic, T. Cavalié, J. C. Loison, and K. M. Hickson. A photochemical model of Triton's atmosphere paired with an uncertainty propagation study. *A&A*, 667:A169, November 2022.
2. Tanguy Bertrand and François Forget. 3D modeling of organic haze in Pluto's atmosphere. *Icarus*, 287:72–86, May 2017.
3. A. L. Broadfoot, S. K. Atreya, J. L. Bertaux, J. E. Blamont, A. J. Dessler, T. M. Donahue, W. T. Forrester, D. T. Hall, F. Herbert, J. B. Holberg, D. M. Hunten, V. A. Krasnopolsky, S. Linick, J. I. Lunine, J. C. McConnell, H. W. Moos, B. R. Sandel, N. M. Schneider, D. E. Shemansky, G. R. Smith, D. F. Strobel, and R. V. Yelle. Ultraviolet Spectrometer Observations of Neptune and Triton. *Science*, 246(4936):1459–1466, December 1989.
4. M. Cabane, P. Rannou, E. Chassefiere, and G. Israel. Fractal aggregates in Titan's atmosphere. *Planet. Space Sci.*, 41(4):257–267, April 1993.
5. Sihe Chen, Eliot F. Young, Leslie A. Young, Tanguy Bertrand, François Forget, and Yuk L. Yung. Global climate model occultation lightcurves tested by August 2018 ground-based stellar occultation. *Icarus*, 356:113976, March 2021.
6. A. F. Cheng, M. E. Summers, G. R. Gladstone, D. F. Strobel, L. A. Young, P. Lavvas, J. A. Kammer, C. M. Lisse, A. H. Parker, E. F. Young, S. A. Stern, H. A. Weaver, C. B. Olkin, and K. Ennico. Haze in Pluto's atmosphere. *Icarus*, 290:112–133, July 2017.
7. A. J. Coates, F. J. Crary, G. R. Lewis, D. T. Young, J. H. Waite, and E. C. Sittler. Discovery of heavy negative ions in Titan's ionosphere. *Geophys. Res. Lett.*, 34(22):L22103, November 2007.
8. B. Conrath, F. M. Flasar, R. Hanel, V. Kunde, W. Maguire, J. Pearl, J. Pirraglia, R. Samuelson, P. Gierasch, A. Weir, B. Bezard, D. Gautier, D. Cruikshank, L. Horn, R. Springer, and W. Shaffer. Infrared Observations of the Neptunian System. *Science*, 246(4936):1454–1459, December 1989.
9. F. J. Crary, B. A. Magee, K. Mandt, J. H. Waite, J. Westlake, and D. T. Young. Heavy ions, temperatures and winds in Titan's ionosphere: Combined Cassini CAPS and INMS observations. *Planet. Space Sci.*, 57(14-15):1847–1856, December 2009.
10. D. P. Cruikshank and P. M. Silvggio. The surface and atmosphere of Pluto. *Icarus*, 41(1):96–102, January 1980.
11. Daniel B. Curtis, Courtney D. Hatch, Christa A. Hasenkopf, Owen B. Toon, Margaret A. Tolbert, Christopher P. McKay, and Bishun N. Khare. Laboratory studies of methane and ethane adsorption and nucleation onto organic particles: Application to Titan's clouds. *Icarus*, 195(2):792–801, June 2008.
12. Vasili Dimitrov and Akiva Bar-Nun. Aging of Titan's Aerosols. *Icarus*, 156(2):530–538, April 2002.
13. J. L. Elliot, A. Ates, B. A. Babcock, A. S. Bosh, M. W. Buie, K. B. Clancy, E. W. Dunham, S. S. Eikenberry, D. T. Hall, S. D. Kern, S. K. Leggett, S. E. Levine, D. S. Moon, C. B. Olkin, D. J. Osip, J. M. Pasachoff, B. E. Penprase, M. J. Person, S. Qu, J. T. Rayner, L. C. Roberts, C. V. Salyk, S. P. Souza, R. C. Stone, B. W. Taylor, D. J. Tholen, J. E. Thomas-Osip, D. R. Ticehurst, and L. H. Wasserman. The recent expansion of Pluto's atmosphere. *Nature*, 424(6945):165–168, July 2003.
14. J. L. Elliot, E. W. Dunham, A. S. Bosh, S. M. Slivan, L. A. Young, L. H. Wasserman, and R. L. Millis. Pluto's atmosphere. *Icarus*, 77(1):148–170, January 1989.
15. J. L. Elliot, M. J. Person, and S. Qu. Analysis of Stellar Occultation Data. II. Inversion, with Application to Pluto and Triton. *AJ*, 126(2):1041–1079, August 2003.
16. J. L. Elliot and L. A. Young. Analysis of Stellar Occultation Data for Planetary Atmospheres. I. Model Fitting Application to Pluto. *AJ*, 103:991, March 1992.
17. Siteng Fan, Peter Gao, Xi Zhang, Danica J. Adams, Nicholas W. Kutsop, Carver J. Bierson, Chao Liu, Jiani Yang, Leslie A. Young, Andrew F. Cheng, and Yuk L. Yung. A bimodal distribution of haze in Pluto's atmosphere. *Nature Communications*, 13:240, January 2022.
18. N. Fray and B. Schmitt. Sublimation of ices of astrophysical interest: A bibliographic review. *Planet. Space Sci.*, 57(14-15):2053–2080, December 2009.
19. Richard G. French, Anthony D. Toigo, Peter J. Gierasch, Candice J. Hansen, Leslie A. Young, Bruno Sicardy, Alex Dias-Oliveira, and Scott D. Guzewich. Seasonal variations in Pluto's atmospheric tides. *Icarus*, 246:247–267, January 2015.
20. Marina Galand, Roger Yelle, Jun Cui, Jan-Erik Wahlund, Véronique Vuitton, Anne Wellbrock, and Andrew Coates. Ionization sources in Titan's deep ionosphere. *Journal of Geophysical Research (Space Physics)*, 115(A7):A07312, July 2010.
21. Peter Gao, Siteng Fan, Michael L. Wong, Mao-Chang Liang, Run-Lie Shia, Joshua A. Kammer, Yuk L. Yung, Michael E. Summers, G. Randall Gladstone, Leslie A. Young, Catherine B. Olkin, Kimberly Ennico, Harold A. Weaver, S. Alan Stern, and New Horizons Science Team. Constraints on the microphysics of Pluto's photochemical haze from New Horizons observations. *Icarus*, 287:116–123, May 2017.

22. G. Randall Gladstone, S. Alan Stern, Kimberly Ennico, Catherine B. Olkin, Harold A. Weaver, Leslie A. Young, Michael E. Summers, Darrell F. Strobel, David P. Hinson, Joshua A. Kammer, Alex H. Parker, Andrew J. Steffl, Ivan R. Linscott, Joel Wm. Parker, Andrew F. Cheng, David C. Slater, Maarten H. Versteeg, Thomas K. Greathouse, Kurt D. Retherford, Henry Throop, Nathaniel J. Cunningham, William W. Woods, Kelsi N. Singer, Constantine C. C. Tsang, Rebecca Schindhelm, Carey M. Lisse, Michael L. Wong, Yuk L. Yung, Xun Zhu, Werner Curdt, Panayotis Lavvas, Eliot F. Young, G. Leonard Tyler, F. Bagenal, W. M. Grundy, W. B. McKinnon, J. M. Moore, J. R. Spencer, T. Andert, J. Andrews, M. Banks, B. Bauer, J. Bauman, O. S. Barnouin, P. Bedini, K. Beisser, R. A. Beyer, S. Bhaskaran, R. P. Binzel, E. Birath, M. Bird, D. J. Bogan, A. Bowman, V. J. Bray, M. Brozovic, C. Bryan, M. R. Buckley, M. W. Buie, B. J. Buratti, S. S. Bushman, A. Calloway, B. Carcich, S. Conard, C. A. Conrad, J. C. Cook, D. P. Cruikshank, O. S. Custodio, C. M. Dalle Ore, C. Deboy, Z. J. B. Dischner, P. Dumont, A. M. Earle, H. A. Elliott, J. Ercol, C. M. Ernst, T. Finley, S. H. Flanigan, G. Fountain, M. J. Freeze, J. L. Green, Y. Guo, M. Hahn, D. P. Hamilton, S. A. Hamilton, J. Hanley, A. Harch, H. M. Hart, C. B. Hersman, A. Hill, M. E. Hill, M. E. Holdridge, M. Horanyi, A. D. Howard, C. J. A. Howett, C. Jackman, R. A. Jacobson, D. E. Jennings, H. K. Kang, D. E. Kaufmann, P. Kollmann, S. M. Krimigis, D. Kusnierkiewicz, T. R. Lauer, J. E. Lee, K. L. Lindstrom, A. W. Lunsford, V. A. Mallder, N. Martin, D. J. McComas, R. L. McNutt, D. Mehoke, T. Mehoke, E. D. Melin, M. Mutchler, D. Nelson, F. Nimmo, J. I. Nunez, A. Ocampo, W. M. Owen, M. Paetzold, B. Page, F. Pelletier, J. Peterson, N. Pinkine, M. Piquette, S. B. Porter, S. Protopapa, J. Redfern, H. J. Reitsema, D. C. Reuter, J. H. Roberts, S. J. Robbins, G. Rogers, D. Rose, K. Runyon, M. G. Ryschlewitsch, P. Schenk, B. Sepan, M. R. Showalter, M. Soluri, D. Stanbridge, T. Stryk, J. R. Szalay, M. Tapley, A. Taylor, H. Taylor, O. M. Umurhan, A. J. Verbiscer, M. H. Versteeg, M. Vincent, R. Webbert, S. Weidner, G. E. Weigle, O. L. White, K. Whittenburg, B. G. Williams, K. Williams, S. Williams, A. M. Zangari, and E. Zirnstein. The atmosphere of Pluto as observed by New Horizons. *Science*, 351(6279):aad8866, March 2016.
23. W. M. Grundy, T. Bertrand, R. P. Binzel, M. W. Buie, B. J. Buratti, A. F. Cheng, J. C. Cook, D. P. Cruikshank, S. L. Devins, C. M. Dalle Ore, A. M. Earle, K. Ennico, F. Forget, P. Gao, G. R. Gladstone, C. J. A. Howett, D. E. Jennings, J. A. Kammer, T. R. Lauer, I. R. Linscott, C. M. Lisse, A. W. Lunsford, W. B. McKinnon, C. B. Olkin, A. H. Parker, S. Protopapa, E. Quirico, D. C. Reuter, B. Schmitt, K. N. Singer, J. A. Spencer, S. A. Stern, D. F. Strobel, M. E. Summers, H. A. Weaver, G. E. Weigle, M. L. Wong, E. F. Young, L. A. Young, and X. Zhang. Pluto’s haze as a surface material. *Icarus*, 314:232–245, November 2018.
24. A. A. S. Gulbis, J. P. Emery, M. J. Person, A. S. Bosh, C. A. Zuluaga, J. M. Pasachoff, and B. A. Babcock. Observations of a successive stellar occultation by Charon and graze by Pluto in 2011: Multiwavelength SpeX and MORIS data from the IRTF. *Icarus*, 246:226–236, January 2015.
25. Mark A. Gurwell. Submillimeter Observations of Titan: Global Measures of Stratospheric Temperature, CO, HCN, HC<sub>3</sub>N, and the Isotopic Ratios <sup>12</sup>C/<sup>13</sup>C and <sup>14</sup>N/<sup>15</sup>N. *ApJL*, 616(1):L7–L10, November 2004.
26. Chao He, Sarah M. Hörst, Sydney Riemer, Joshua A. Sebree, Nicholas Pauley, and Véronique Vuitton. Carbon Monoxide Affecting Planetary Atmospheric Chemistry. *ApJL*, 841(2):L31, June 2017.
27. Floyd Herbert and B. R. Sandel. CH<sub>4</sub> and haze in Triton’s lower atmosphere. *J. Geophys. Res.*, 96:19241–19252, October 1991.
28. J. Hillier, P. Helfenstein, A. Verbiscer, and J. Veverka. Voyager photometry of Triton: Haze and surface photometric properties. *J. Geophys. Res.*, 96:19203–19209, October 1991.
29. J. Hillier, P. Helfenstein, A. Verbiscer, J. Veverka, R. H. Brown, J. Goguen, and T. V. Johnson. Voyager Disk-Integrated Photometry of Triton. *Science*, 250(4979):419–421, October 1990.
30. J. Hillier and J. Veverka. Photometric Properties of Triton Hazes. *Icarus*, 109(2):284–295, June 1994.
31. J. H. Hillier, B. J. Buratti, J. D. Hofgartner, M. D. Hicks, S. Devins, and L. Kivrak. Characteristics of Pluto’s Haze and Surface from an Analytic Radiative Transfer Model. *PSJ*, 2(1):11, February 2021.
32. D. P. Hinson, I. R. Linscott, D. F. Strobel, G. L. Tyler, M. K. Bird, M. Pätzold, M. E. Summers, S. A. Stern, K. Ennico, G. R. Gladstone, C. B. Olkin, H. A. Weaver, W. W. Woods, L. A. Young, and New Horizons Science Team. An upper limit on Pluto’s ionosphere from radio occultation measurements with New Horizons. *Icarus*, 307:17–24, June 2018.
33. W. B. Hubbard, D. M. Hunten, S. W. Dieters, K. M. Hill, and R. D. Watson. Occultation evidence for an atmosphere on Pluto. *Nature*, 336(6198):452–454, December 1988.
34. W. B. Hubbard, R. V. Yelle, and J. I. Lunine. Nonisothermal Pluto atmosphere models. *Icarus*, 84(1):1–11, March 1990.
35. Adam D. Jacobs, Michael E. Summers, Andrew F. Cheng, G. Randall Gladstone, Carey M. Lisse, W. Dean Pesnell, Tanguy Bertrand, Darrell F. Strobel, Leslie A. Young, Harold A. Weaver, Joshua Kammer, and Peter Gao. LORRI observations of waves in Pluto’s atmosphere. *Icarus*, 356:113825, March 2021.

36. Perianne E. Johnson, Leslie A. Young, Silvia Protopapa, Bernard Schmitt, Leila R. Gabasova, Briley L. Lewis, John A. Stansberry, Kathy E. Mandt, and Oliver L. White. Modeling Pluto's minimum pressure: Implications for haze production. *Icarus*, 356:114070, March 2021.
37. Lora Jovanović, Thomas Gautier, Laurent Broch, Silvia Protopapa, Tanguy Bertrand, Pascal Rannou, Marie Fayolle, Eric Quirico, Luc Johann, Aotmane En Naciri, and Nathalie Carrasco. Optical constants of Pluto aerosol analogues from UV to near-IR. *Icarus*, 362:114398, July 2021.
38. Lora Jovanović, Thomas Gautier, Véronique Vuitton, Cédric Wolters, Jérémy Bourgalais, Arnaud Buch, François-Régis Orthous-Daunay, Ludovic Vettier, Laurène Flandinet, and Nathalie Carrasco. Chemical composition of Pluto aerosol analogues. *Icarus*, 346:113774, August 2020.
39. Joshua A. Kammer, G. Randall Gladstone, Leslie A. Young, Andrew J. Steffl, Joel W. Parker, Thomas K. Greathouse, Kurt D. Retherford, Maarten H. Versteeg, Darrell F. Strobel, Michael E. Summers, S. Alan Stern, Catherine B. Olkin, Harold A. Weaver, Kimberly Ennico, The New Horizons Atmospheres, and Alice UV Spectrograph Teams. New Horizons Observations of an Ultraviolet Stellar Occultation and Appulse by Pluto's Atmosphere. *AJ*, 159(1):26, January 2020.
40. V. A. Krasnopolsky, B. R. Sandel, and F. Herbert. Properties of haze in the atmosphere of Triton. *J. Geophys. Res.*, 97(E7):11695–11700, July 1992.
41. Vladimir A. Krasnopolsky. Titan's photochemical model: Further update, oxygen species, and comparison with Triton and Pluto. *Planet. Space Sci.*, 73(1):318–326, December 2012.
42. Vladimir A. Krasnopolsky. A photochemical model of Pluto's atmosphere and ionosphere. *Icarus*, 335:113374, January 2020.
43. Vladimir A. Krasnopolsky and Dale P. Cruikshank. Photochemistry of Triton's atmosphere and ionosphere. *J. Geophys. Res.*, 100(E10):21271–21286, January 1995.
44. N. W. Kutsop, A. G. Hayes, B. J. Buratti, P. M. Corlies, K. Ennico, S. Fan, R. Gladstone, P. Helfenstein, J. D. Hofgartner, M. Hicks, M. Lemmon, J. I. Lunine, J. Moore, C. B. Olkin, A. H. Parker, S. A. Stern, H. A. Weaver, L. A. Young, and The New Horizons Science Team. Pluto's Haze Abundance and Size Distribution from Limb Scatter Observations by MVIC. *PSJ*, 2(3):91, June 2021.
45. L. M. Lara, W. H. Ip, and R. Rodrigo. Photochemical Models of Pluto's Atmosphere. *Icarus*, 130(1):16–35, November 1997.
46. P. Lavvas, E. Lellouch, D. F. Strobel, M. A. Gurwell, A. F. Cheng, L. A. Young, and G. R. Gladstone. A major ice component in Pluto's haze. *Nature Astronomy*, 5:289–297, January 2021.
47. P. Lavvas, R. V. Yelle, and C. A. Griffith. Titan's vertical aerosol structure at the Huygens landing site: Constraints on particle size, density, charge, and refractive index. *Icarus*, 210(2):832–842, December 2010.
48. Panayotis Lavvas, Roger V. Yelle, Tommi Koskinen, Axel Bazin, Véronique Vuitton, Erik Vigren, Marina Galand, Anne Wellbrock, Andrew J. Coates, Jan-Erik Wahlund, Frank J. Cray, and Darci Snowden. Aerosol growth in titan's ionosphere. *Proceedings of the National Academy of Sciences*, 110(8):2729–2734, 2013.
49. E. Lellouch, C. de Bergh, B. Sicardy, S. Ferron, and H. U. Käufl. Detection of CO in Triton's atmosphere and the nature of surface-atmosphere interactions. *A&A*, 512:L8, March 2010.
50. E. Lellouch, C. de Bergh, B. Sicardy, H. U. Käufl, and A. Smette. High resolution spectroscopy of Pluto's atmosphere: detection of the 2.3  $\mu\text{m}$  CH<sub>4</sub> bands and evidence for carbon monoxide. *A&A*, 530:L4, June 2011.
51. E. Lellouch, M. Gurwell, B. Butler, T. Fouchet, P. Lavvas, D. F. Strobel, B. Sicardy, A. Moullet, R. Moreno, D. Bockelée-Morvan, N. Biver, L. Young, D. Lis, J. Stansberry, A. Stern, H. Weaver, E. Young, X. Zhu, and J. Boissier. Detection of CO and HCN in Pluto's atmosphere with ALMA. *Icarus*, 286:289–307, April 2017.
52. Adrienn Luspay-Kuti, Kathleen Mandt, Kandis-Lea Jessup, Joshua Kammer, Vincent Hue, Mark Hamel, and Rachael Filwett. Photochemistry on Pluto - I. Hydrocarbons and aerosols. *MNRAS*, 472(1):104–117, November 2017.
53. T. Majeed, J. C. McConnell, D. F. Strobel, and M. E. Summers. The ionosphere of Triton. *Geophys. Res. Lett.*, 17(10):1721–1724, September 1990.
54. Kathleen Mandt, Adrienn Luspay-Kuti, Mark Hamel, Kandis-Lea Jessup, Vincent Hue, Josh Kammer, and Rachael Filwett. Photochemistry on Pluto: part II HCN and nitrogen isotope fractionation. *MNRAS*, 472(1):118–128, November 2017.
55. Gene D. McDonald, W. R. Thompson, Michael Heinrich, Bishun N. Khare, and Carl Sagan. Chemical Investigation of Titan and Triton Tholins. *Icarus*, 108(1):137–145, March 1994.
56. R. L. Millis, L. H. Wasserman, O. G. Franz, R. A. Nye, J. L. Elliot, E. W. Dunham, A. S. Bosh, L. A. Young, S. M. Slivan, A. C. Gilmore, P. M. Kilmartin, W. H. Allen, R. D. Watson, S. W. Dieters, K. M. Hill, A. B. Giles, G. Blow, J. Priestley, W. M. Kissling, W. S. G. Walker, B. F. Marino, D. G. Dix, A. A. Page, J. E. Ross, H. P. Avey, D. Hickey, H. D. Kennedy, K. A. Mottram, G. Moyland, T. Murphy, C. C. Dahn, and A. R. Klemola. Pluto's Radius and Atmosphere: Results from the Entire 9 June 1988 Occultation Data Set. *Icarus*, 105(2):282–297, October 1993.

57. Sarah E. Moran, Sarah M. Hörst, Chao He, Michael J. Radke, Joshua A. Sebree, Noam R. Izenberg, Véronique Vuitton, Laurène Flandinet, François-Régis Orthous-Daunay, and Cédric Wolters. Triton Haze Analogs: The Role of Carbon Monoxide in Haze Formation. *Journal of Geophysical Research (Planets)*, 127(1):e06984, January 2022.
58. Julianne I. Moses, Mark Allen, and Yuk L. Yung. Hydrocarbon nucleation and aerosol formation in Neptune’s atmosphere. *Icarus*, 99(2):318–346, October 1992.
59. Kazumasa Ohno, Xi Zhang, Ryo Tazaki, and Satoshi Okuzumi. Haze Formation on Triton. *ApJ*, 912(1):37, May 2021.
60. Catherine B. Olkin, Leslie A. Young, Richard G. French, Eliot F. Young, Marc W. Buie, Robert R. Howell, Jeffrey Regester, Catherine R. Ruhland, Tim Natusch, and David J. Ramm. Pluto’s atmospheric structure from the July 2007 stellar occultation. *Icarus*, 239:15–22, September 2014.
61. T. C. Owen, T. L. Roush, D. P. Cruikshank, J. L. Elliot, L. A. Young, C. de Bergh, B. Schmitt, T. R. Geballe, R. H. Brown, and M. J. Bartholomew. Surface Ices and the Atmospheric Composition of Pluto. *Science*, 261(5122):745–748, August 1993.
62. Jay M. Pasachoff, Steven P. Souza, Bryce A. Babcock, David R. Ticehurst, J. L. Elliot, M. J. Person, K. B. Clancy, Jr. Roberts, Lewis C., D. T. Hall, and David J. Tholen. The Structure of Pluto’s Atmosphere from the 2002 August 21 Stellar Occultation. *AJ*, 129(3):1718–1723, March 2005.
63. M. J. Person, J. L. Elliot, A. A. S. Gulbis, C. A. Zuluaga, B. A. Babcock, A. J. McKay, J. M. Pasachoff, S. P. Souza, W. B. Hubbard, C. A. Kulesa, D. W. McCarthy, S. D. Benecchi, S. E. Levine, A. S. Bosh, E. V. Ryan, W. H. Ryan, A. Meyer, J. Wolf, and J. Hill. Waves in Pluto’s Upper Atmosphere. *AJ*, 136(4):1510–1518, October 2008.
64. James B. Pollack, Joel M. Schwartz, and Kathy Rages. Scatterers in Triton’s Atmosphere: Implications for the Seasonal Volatile Cycle. *Science*, 250(4979):440–443, October 1990.
65. H. R. Pruppacher and J. D. Klett. *Microphysics of clouds and precipitation*. D. Reidel Publishing Company, Dordrecht, Holland, 1978.
66. Kathy Rages and James B. Pollack. Voyager imaging of Triton’s clouds and hazes. *Icarus*, 99(2):289–301, October 1992.
67. K. Ågren, J. E. Wahlund, P. Garnier, R. Modolo, J. Cui, M. Galand, and I. Müller-Wodarg. On the ionospheric structure of Titan. *Planet. Space Sci.*, 57(14-15):1821–1827, December 2009.
68. P. Rannou, D. Curtis, and M. A. Tolbert. Adsorption isotherms and nucleation of methane and ethane on an analog of Titan’s photochemical aerosols. *A&A*, 631:A151, November 2019.
69. P. Rannou and R. West. Supersaturation on Pluto and elsewhere. *Icarus*, 312:36–44, September 2018.
70. Pascal Rannou, Michel Cabane, Robert Botet, and Eric Chassefière. A new interpretation of scattered light measurements at Titan’s limb. *J. Geophys. Res.*, 102(E5):10997–11014, January 1997.
71. B. A. Smith, L. A. Soderblom, D. Banfield, C. Barnet, A. T. Basilevksy, R. F. Beebe, K. Bollinger, J. M. Boyce, A. Brahic, G. A. Briggs, R. H. Brown, C. Chyba, S. A. Collins, T. Colvin, A. F. Cook, D. Crisp, S. K. Croft, D. Cruikshank, J. N. Cuzzi, G. E. Danielson, M. E. Davies, E. de Jong, L. Dones, D. Godfrey, J. Goguen, I. Grenier, V. R. Haemmerle, H. Hammel, C. J. Hansen, C. P. Helfenstein, C. Howell, G. E. Hunt, A. P. Ingersoll, T. V. Johnson, J. Kargel, R. Kirk, D. I. Kuehn, S. Limaye, H. Masursky, A. McEwen, D. Morrison, T. Owen, W. Owen, J. B. Pollack, C. C. Porco, K. Rages, P. Rogers, D. Rudy, C. Sagan, J. Schwartz, E. M. Shoemaker, M. Showalter, B. Sicardy, D. Simonelli, J. Spencer, L. A. Sromovsky, C. Stoker, R. G. Strom, V. E. Suomi, S. P. Synott, R. J. Terrile, P. Thomas, W. R. Thompson, A. Verbiscer, and J. Veverka. Voyager 2 at Neptune: Imaging Science Results. *Science*, 246(4936):1422–1449, December 1989.
72. John A. Stansberry, Jonathan I. Lunine, and Martin G. Tomasko. Upper limits on possible photochemical hazes on Pluto. *Geophys. Res. Lett.*, 16(11):1221–1224, November 1989.
73. S. A. Stern, J. A. Kammer, E. L. Barth, K. N. Singer, T. R. Lauer, J. D. Hofgartner, H. A. Weaver, K. Ennico, C. B. Olkin, L. A. Young, New Horizons LORRI Instrument Team, New Horizons Ralph Instrument Team, and New Horizons Atmospheres Investigation Team. Evidence for Possible Clouds in Pluto’s Present-day Atmosphere. *AJ*, 154(2):43, August 2017.
74. D. F. Strobel and M. E. Summers. Triton’s upper atmosphere and ionosphere. In *Neptune and Triton*, pages 1107–1148, January 1995.
75. Darrell F. Strobel, Michael E. Summers, Floyd Herbert, and Bill R. Sandel. The photochemistry of methane in the atmosphere of Triton. *Geophys. Res. Lett.*, 17(10):1729–1732, September 1990.
76. W. R. Thompson, S. K. Singh, B. N. Khare, and C. Sagan. Triton: Stratospheric molecules and organic sediments. *Geophys. Res. Lett.*, 16(8):981–984, August 1989.
77. Anthony D. Toigo, Richard G. French, Peter J. Gierasch, Scott D. Guzewich, Xun Zhu, and Mark I. Richardson. General circulation models of the dynamics of Pluto’s volatile transport on the eve of the New Horizons encounter. *Icarus*, 254:306–323, July 2015.

78. Kimberly A. Tryka, Robert H. Brown, Dale P. Cruikshank, Tobias C. Owen, Thomas R. Geballe, and Catherine de Bergh. Temperature of Nitrogen Ice on Pluto and Its Implications for Flux Measurements. *Icarus*, 112(2):513–527, December 1994.
79. G. L. Tyler, D. N. Sweetnam, J. D. Anderson, S. E. Borutzki, J. K. Campbell, V. R. Eshleman, D. L. Gresh, E. M. Gurrola, D. P. Hinson, N. Kawashima, E. R. Kursinski, G. S. Levy, G. F. Lindal, J. R. Lyons, E. A. Marouf, P. A. Rosen, R. A. Simpson, and G. E. Wood. Voyager Radio Science Observations of Neptune and Triton. *Science*, 246(4936):1466–1473, December 1989.
80. V. Vuitton, P. Lavvas, R. V. Yelle, M. Galand, A. Wellbrock, G. R. Lewis, A. J. Coates, and J. E. Wahlund. Negative ion chemistry in Titan’s upper atmosphere. *Planet. Space Sci.*, 57(13):1558–1572, November 2009.
81. V. Vuitton, R. V. Yelle, S. J. Klippenstein, S. M. Hörst, and P. Lavvas. Simulating the density of organic species in the atmosphere of Titan with a coupled ion-neutral photochemical model. *Icarus*, 324:120–197, May 2019.
82. R. A. West and P. H. Smith. Evidence for aggregate particles in the atmospheres of Titan and Jupiter. *Icarus*, 90(2):330–333, April 1991.
83. E. H. Wilson and S. K. Atreya. Current state of modeling the photochemistry of Titan’s mutually dependent atmosphere and ionosphere. *Journal of Geophysical Research (Planets)*, 109(E6):E06002, June 2004.
84. Michael L. Wong, Siteng Fan, Peter Gao, Mao-Chang Liang, Run-Lie Shia, Yuk L. Yung, Joshua A. Kammer, Michael E. Summers, G. Randall Gladstone, Leslie A. Young, Catherine B. Olkin, Kimberly Ennico, Harold A. Weaver, S. Alan Stern, and New Horizons Science Team. The photochemistry of Pluto’s atmosphere as illuminated by New Horizons. *Icarus*, 287:110–115, May 2017.
85. E. F. Young, R. G. French, L. A. Young, C. R. Ruhland, M. W. Buie, C. B. Olkin, J. Regester, K. Shoemaker, G. Blow, J. Broughton, G. Christie, D. Gault, B. Lade, and T. Natusch. Vertical Structure in Pluto’s Atmosphere from the 2006 June 12 Stellar Occultation. *AJ*, 136(5):1757–1769, November 2008.
86. Leslie A. Young. Volatile transport on inhomogeneous surfaces: II. Numerical calculations (VT3D). *Icarus*, 284:443–476, March 2017.
87. Leslie A. Young, J. L. Elliot, Alan Tokunaga, Catherine de Bergh, and Tobias Owen. Detection of Gaseous Methane on Pluto. *Icarus*, 127(1):258–262, May 1997.
88. Leslie A. Young, Joshua A. Kammer, Andrew J. Steffl, G. Randall Gladstone, Michael E. Summers, Darrell F. Strobel, David P. Hinson, S. Alan Stern, Harold A. Weaver, Catherine B. Olkin, Kimberly Ennico, David J. McComas, Andrew F. Cheng, Peter Gao, Panayotis Lavvas, Ivan R. Linscott, Michael L. Wong, Yuk L. Yung, Nathaniel Cunningham, Michael Davis, Joel Wm. Parker, Rebecca Schindhelm, Oswald H. W. Siegmund, John Stone, Kurt Retherford, and Maarten Versteeg. Structure and composition of Pluto’s atmosphere from the New Horizons solar ultraviolet occultation. *Icarus*, 300:174–199, January 2018.
89. Xinting Yu, Yue Yu, Julia Garver, Jialin Li, Abigale Hawthorn, Ella Sciamma-O’Brien, Xi Zhang, and Erika Barth. Material Properties of Organic Liquids, Ices, and Hazes on Titan. *arXiv e-prints*, page arXiv:2210.01394, October 2022.
90. Y. L. Yung, M. Allen, and J. P. Pinto. Photochemistry of the atmosphere of Titan - Comparison between model and observations. *ApJS*, 55:465–506, July 1984.
91. Y. L. Yung and J. R. Lyons. Triton: Topside ionosphere and nitrogen escape. *Geophys. Res. Lett.*, 17(10):1717–1720, September 1990.
92. Xi Zhang, Darrell F. Strobel, and Hiroshi Imanaka. Haze heats Pluto’s atmosphere yet explains its cold temperature. *Nature*, 551(7680):352–355, November 2017.